Clinical Trial/Experimental Study

Medicine®

OPEN

The imaging features of the meniscal roots on isotropic 3D MRI in young asymptomatic volunteers

Ping Wang, MD[a], Cheng-Zhou Zhang, MD[a], Di Zhang, MD[a], Quan-Yuan Liu, MD[a], Xiao-Fei Zhong, MD[a], Zhi-Jie Yin, MD[a], Bin Wang, MD, PhD[b,*]

Abstract

Background: This study aimed to describe clearly the normal imaging features of the meniscal roots on the magnetic resonance imaging (MRI) with a 3-dimensional (3D) proton density-weighted (PDW) sequence at 3T.

Methods: A total of 60 knees of 31 young asymptomatic volunteers were examined using a 3D MRI. The insertion patterns, constitution patterns, and MR signals of the meniscal roots were recorded.

Results: The anterior root of the medial meniscus (ARMM), the anterior root of the lateral meniscus (ARLM), and the posterior root of the medial meniscus (PRMM) had 1 insertion site, whereas the posterior root of the lateral meniscus (PRLM) can be divided into major and minor insertion sites. The ARLM and the PRMM usually consisted of multiple fiber bundles (≥3), whereas the ARMM and the PRLM often consisted of a single fiber bundle. The ARMM and the PRLM usually appeared as hypointense, whereas the ARLM and the PRMM typically exhibited mixed signals.

Conclusions: The meniscal roots can be complex and diverse, and certain characteristics of them were observed on 3D MRI. Understanding the normal imaging features of the meniscal roots is extremely beneficial for further diagnosis of root tears.

Abbreviations: ARLM = anterior root of the lateral meniscus, ARMM = anterior root of the medial meniscus, MRI = magnetic resonance imaging, MRT = meniscal root tear, PDW = proton density-weighted, PRLM = posterior root of the lateral meniscus, PRMM = posterior root of the medial meniscus, SPACE = sampling perfection with application-optimized contrasts using different flip angle evolutions, TSE = turbo spin echo.

Keywords: anatomy, knee, meniscus, MRI, root

1. Introduction

Meniscal roots of the knee, including the anterior root of the medial meniscus (ARMM), the anterior root of the lateral meniscus (ARLM), the posterior root of the medial meniscus (PRMM), and the posterior root of the lateral meniscus (PRLM), originate from the anterior and posterior horns of the menisci and anchor the menisci to the tibia.[1] The meniscal roots are critical in maintaining the normal biomechanical functions of the menisci.[2] Several biomechanical studies had revealed that the effect of a meniscal root tear (MRT) was functionally equivalent to that of a total meniscectomy,[3,4] and the proper placement of the meniscal root attachment was critical to restoring meniscal function.[5,6] Thus, the accurate diagnosis of MRTs at the early stage is important.

Magnetic resonance imaging (MRI) with its high soft tissue contrast had been the only noninvasive adjunct for diagnosing MRTs during preoperative planning.[7–10] Understanding the normal imaging features of the meniscal roots was a prerequisite to diagnose MRTs, whereas only few studies[11,12] had revealed the anatomy of the meniscal roots with MRI, and several deficiencies exist. First, 1 previous study used the routine MR sequence with a section thickness ≥2.5 mm.[12] Thick sections can lead to an average volume because the meniscal roots are small, affecting the accuracy of the observations. Second, the study objects in previous studies were patients, and the imaging features of the meniscal roots in young asymptomatic volunteers have not been studied, which can reduce selection bias from degenerative process or anatomical anomaly when relatively older people were included.[11,12] Third, we found in the clinical work that the meniscal roots can consist of diverse number of constitution fiber bundles on MR, and the constitution patterns of the meniscal roots have not been studied previously to our knowledge.

The 2-dimensional (2D) turbo spin echo (TSE) proton density-weighted (PDW) sequence, which provides better contrast with the surrounding articular cartilage, tendons, ligaments, menisci, and joint fluid, has been widely accepted as the first choice in

Editor: Weisheng Zhang.

PW and C-ZZ contributed equally to this paper.

The authors declare that there are no conflicts of interest.

[a] Department of Radiology, The Affiliated Hospital of Binzhou Medical University, School of Medicine, Binzhou Medical University, Binzhou, [b] Medical Imaging Research Institute, Department of Radiology, School of Medicine, Binzhou Medical University, Yantai, Shandong, China.

[*] Correspondence: Bin Wang, Medical Imaging Research Institute, Department of Radiology, School of Medicine, Binzhou Medical University, No. 346, Guanhai Rd, Yantai, Shandong 264003, China (e-mail: binwang001@aliyun.com).

Medicine (2018) 97:18(e0624)

Received: 4 November 2017 / Accepted: 11 April 2018

http://dx.doi.org/10.1097/MD.0000000000010624

clinic for the internal derangements of the knee.[7,8] Three-dimensional (3D) MRI offers several potential improvements upon 2D MRI, including improved spatial resolution and the facilitation of interactive 3D visualization and multiplanar reconstructions in any imaging plane, which is advantageous in evaluating small and complex structures. In contrast to rapid 3D gradient echo techniques, the single-slab 3D proton-density, TSE sampling perfection with application-optimized contrasts using variable flip-angle evolution (SPACE) sequence can produce TSE PDW contrast images, which is best suited for studying the anatomy of the meniscal roots.[11,13] This study aimed to describe further the imaging features of the normal meniscal roots in young asymptomatic volunteers with an isotropic 3D PD-SPACE sequence.

2. Materials and methods

2.1. Study population

All the human subjects provided informed consent to participate in the research, which was approved by our institutional review board. A total of 60 knees from 31 volunteers (2 volunteers underwent scanning of one side of the knee, 13 male and 18 female, mean age was 22 years, age range was 20–23 years) were scanned by 3D MRI from October, 2015 to February, 2016. Only volunteers with normal body mass index, and with no symptoms and no history of injury, infection, synovitis, or arthritis of the knee were included in the study.

2.2. MR data acquisition

All examinations were performed with a 3.0-T MR scanner (Magnetom Skyra with TIM system; Siemens Healthcare, Erlangen, Germany) and a dedicated knee coil with an 8-channel receiver. The volunteers were examined in the supine position, with their knees in the knee coil in extension position. An isotropic fat-suppressed 3D PD-SPACE sequence (TR/TE = 1200 ms/28 ms, section thickness/interslice gap = 0.6 mm/0 mm, NEX = 1, field of view, 150 mm × 160 mm; matrix, 256 × 256; and voxel size, 0.6 mm × 0.6 mm × 0.6 mm) was obtained from all volunteers. The scanning time for this sequence was 8 minutes 53 seconds.

2.3. Image analysis

Image analysis was performed on a picture archiving and communication system workstation (GE Advantage Workstation 4.3). A dynamic 3D interactive visualization model was used to evaluate the 4 meniscal roots. All MR studies were reviewed by 2 radiologists (with 11 and 10 years of subspecialty expertise in musculoskeletal MRI) in consensus.

The insertion patterns, constitution patterns, and MR signals of the meniscal roots were reviewed in the combined axial, coronal, and sagittal planes. The insertion patterns of the meniscal roots were classified into different types depending on the insertion area on the tibial plateau. The constitution patterns of the meniscal roots were divided into different types depending on the diverse number of constitution fiber bundles inserted on the tibial plateau. The MR signals of the meniscal roots were divided into hypointense (the signal intensity of the meniscal roots was low and homogenous), mixed signals (the signal intensity of the meniscal roots was mixed with low and high signal intensities), and hyperintense (the signal intensity of the meniscal roots was diffusely higher than that of the other parts of the meniscus). A stripe-like signal, defined as low signal intensity alternating with high signal intensity, resembling the teeth of a comb, was included in the mixed signal.

3. Results

3.1. Insertion patterns of the meniscal roots

The insertion patterns of the meniscal roots were classified in Table 1.

The ARMM (Fig. 1), the ARLM (Fig. 2), and the PRMM (Figs. 3–5) had 1 insertion site, whereas the PRLM (Fig. 6) can be divided into major and minor insertion sites.

3.2. Constitution patterns of the meniscal roots

The constitution patterns of the meniscal roots are classified in Table 2.

The ARLM (Fig. 2) and the PRMM (Fig. 3) usually consisted of multiple fiber bundles (≥3), whereas the ARMM (Fig. 1) and the major and minor components of the PRLM (Figs. 6 and 7) often consisted of a single fiber bundle.

3.3. MR signals of the meniscal roots

The MR signals of the meniscal roots are presented in Table 3.

The ARMM (Fig. 1) and the PRLM (Figs. 6 and 7) usually appeared as hypointense, whereas the ARLM (Fig. 2) and the PRMM (Figs. 3 and 5) typically exhibited mixed signals (most of which were stripe-like signals).

Table 1

Insertion patterns of the meniscal roots on 3D PDW SPACE.

Meniscal root	Pattern	Insertion patterns	Percentage
ARMM	Type I	One insertion site: on the front end of the tibial plateau (Fig. 1)	58 (96.7%)
	Type II	No insertion site on the tibial plateau; the transverse genual ligament was observed	2 (3.3%)
ARLM		One insertion site: on the front area of the intertubercular fossa and lateral to the tibial insertion site of the anterior cruciate ligament (Fig. 2)	60 (100%)
PRMM		One insertion site: on the posterior slope of the medial tibial tubercle (Figs. 3–5)	60 (100%)
PRLM	Type I	One insertion site: on the medial tibial tubercle along the intertubercular fossa (Fig. 7)	32 (53.3%)
	Type II	Two insertion sites: the major component on the medial tibial tubercle along the intertubercular fossa and the minor component on the posterior slope of the lateral tibial tubercle (Fig. 6)	28 (46.7%)

3D = 3-dimensional, ARLM = anterior root of the lateral meniscus, ARMM = anterior root of the medial meniscus, PDW = proton density-weighted, PRLM = posterior root of the lateral meniscus, PRMM = posterior root of the medial meniscus, SPACE = sampling perfection with application-optimized contrasts using different flip angle evolutions.

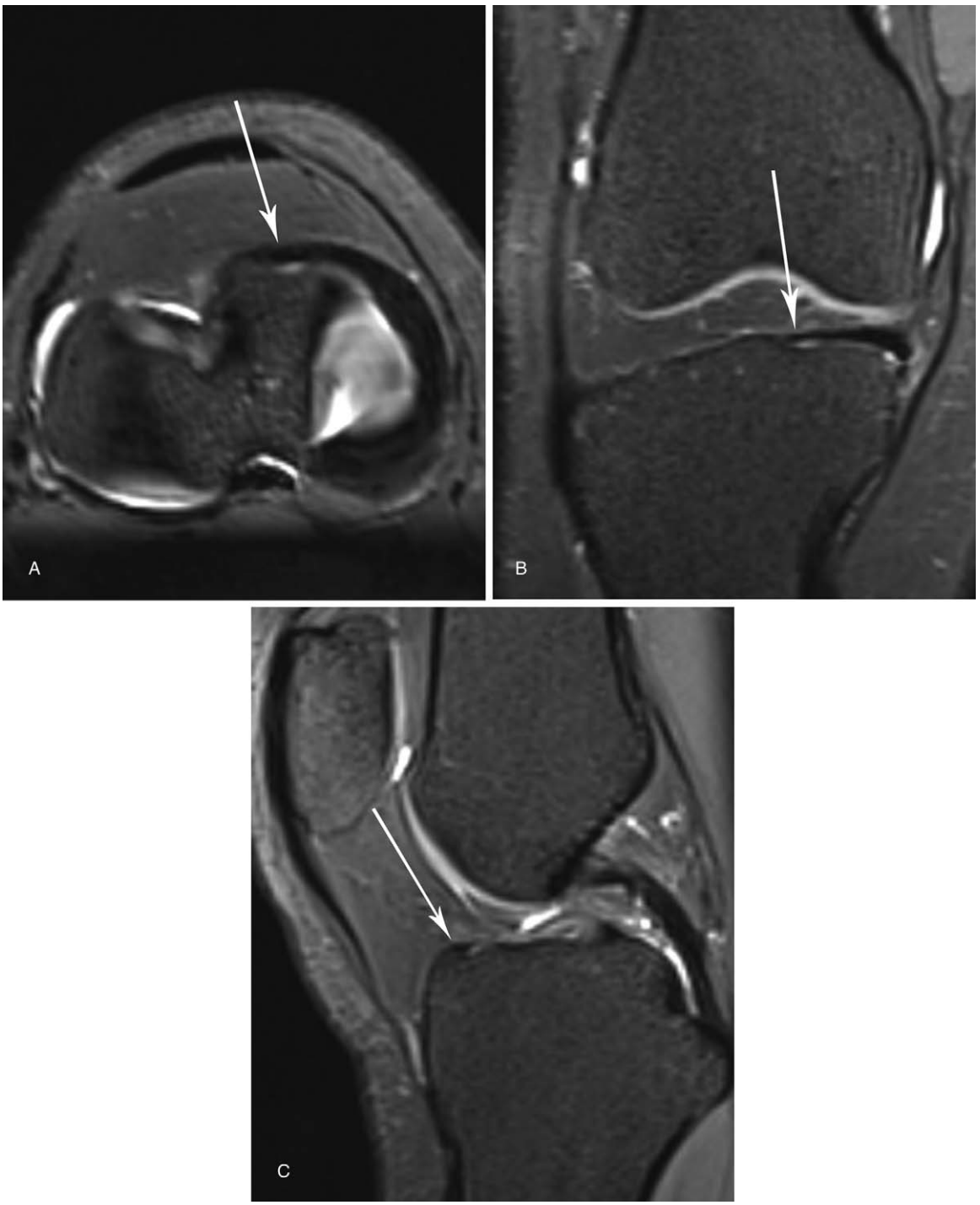

Figure 1. Anterior root of the medial meniscus (ARMM). (A) Axial; (B) coronal; and (C) sagittal images reveal that the ARMM (white arrow) consisted of a single fiber bundle, appeared as hypointense, and inserted on the front end of the tibial plateau.

4. Discussion

Currently, the anatomical study of the meniscal roots mainly included cadaveric study, arthroscopy, and MRI.[1,11,12,14–16] Some meniscal roots, such as the PRLM, had been difficult to visualize fully both on the cadaveric knee specimens and by arthroscopy, because of their unique configuration and position.[7,15,16] Thus, imaging anatomy was an effective supplement for gross and arthroscopic anatomy.

The insertion patterns of the ARMM, the ARLM, and the PRMM were fixed, whereas the PRLM had relatively more complex insertion patterns. The ARMM was inserted on the anterior edge of the tibial plateau; the ARLM was inserted on the front area of the intertubercular fossa; and the PRMM was inserted on the posterior slope of the medial tibial tubercle, which were in accordance with previous studies.[1,11,14,16] The PRLM was divided into the major component, which was inserted on the medial tibial tubercle along the intertubercular fossa, and the

Figure 2. Anterior root of the lateral meniscus (ARLM). (A) Axial; (B) coronal; and (C) sagittal images reveal that the ARLM (white arrow) consisted of multiple fiber bundles, appeared as mixed signal, and inserted on the front area of the intercondylar fossa.

minor component, which was inserted on the posterior slope of the lateral tibial tubercle in this study, which was in accordance with previous studies.[4,12,14] For the major component of the PRLM, differential diagnosis with displaced meniscal fragment, such as a bucket handle tear or flap tear, should be conducted on MR images, because it follows a long course along the intertubercular crest. In the current study, the 46.7% of the PRLM had the minor insertion site was found. The minor root attachment was separated from the posterior of the major root attachment, and the separation area had potential pitfalls for the misinterpretation of MRTs should be noticed by radiologists.

The constitution patterns of the meniscal roots have not been systematically reported previously to our knowledge. The ARLM and the PRMM usually consisted of multiple fiber bundles (≥3), whereas the ARMM, and the major and minor components of the PRLM often consisted of a single fiber bundle. The multiple

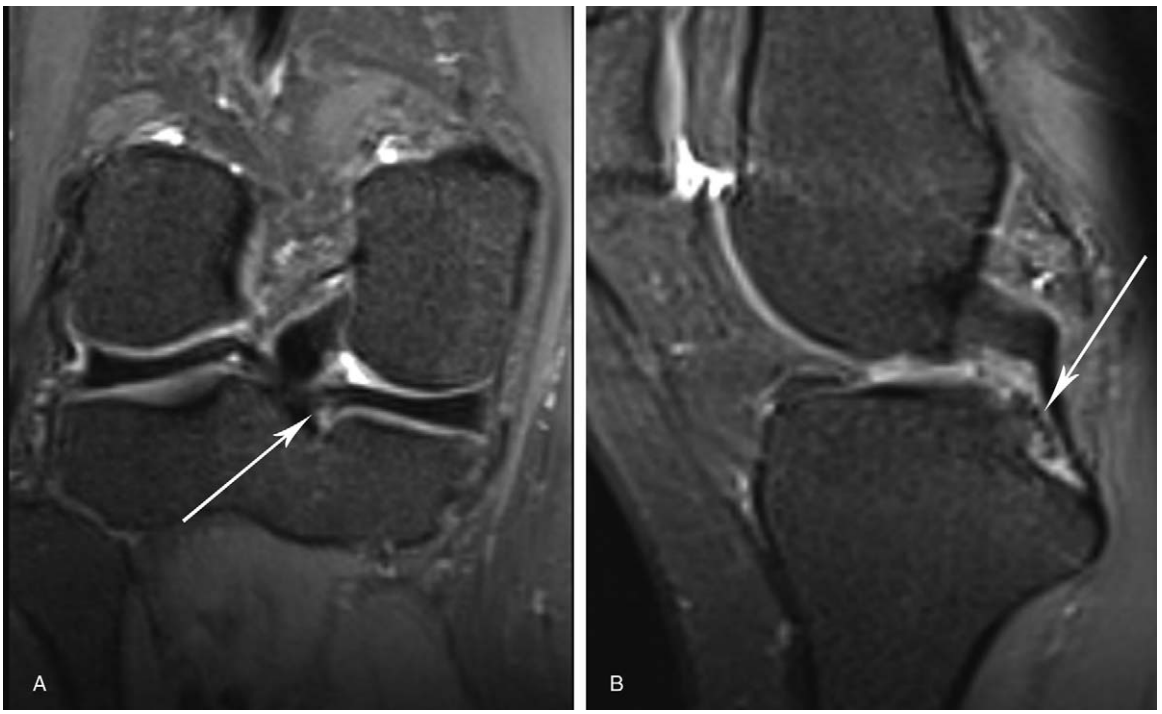

Figure 3. Posterior root of the medial meniscus (PRMM). (A) Coronal; and (B) sagittal images reveal that the PRMM (white arrow) consisted of multiple fiber bundles, appeared as stripe-like signals, and inserted on the posterior slope of the medial tibial tubercle.

numbers of constitution fiber bundles of the meniscal roots may be attributed to the following reasons. First, the meniscal roots actually consisted of multiple fiber bundles. Previous arthroscopic studies of the PRMM[14,17] reported the appearance of "shiny white fibers," a posterior-based sheet of supplemental fibers continuous with the main root attachment. Second, the internal inherent components along the course of the meniscal roots, which can appear as high signal intensity on the PDW sequence, may be present, making the meniscal roots seem to consist of multiple fiber bundles. The constitution patterns of the meniscal

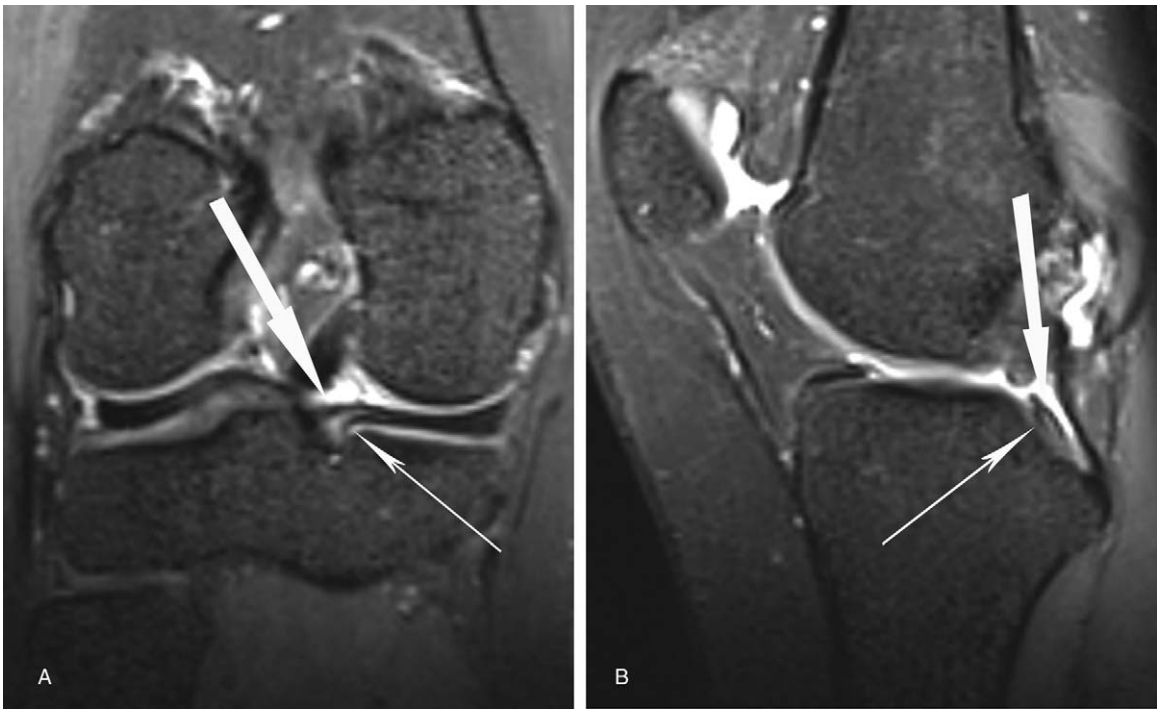

Figure 4. Posterior root of the medial meniscus (PRMM). (A) Coronal; and (B) sagittal images reveal that the PRMM (thick and thin, white arrow) consisted of 2 fiber bundles, appeared as hypointense, and inserted on the posterior slope of the medial tibial tubercle.

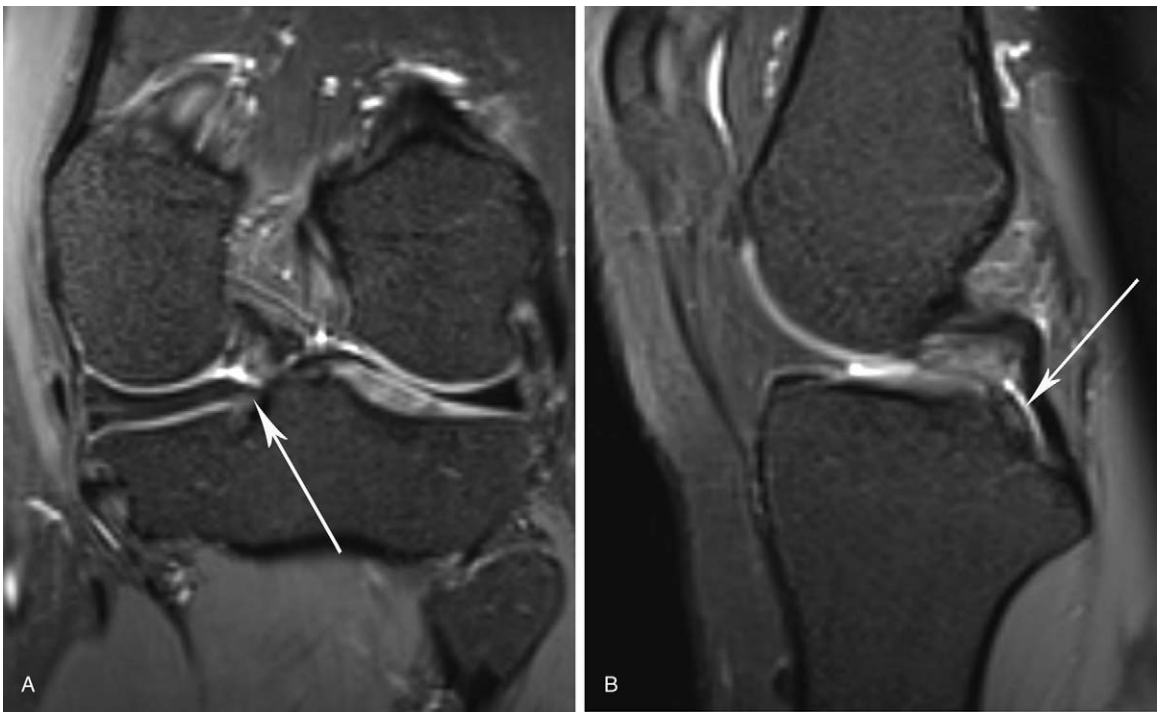

Figure 5. Posterior root of the medial meniscus (PRMM). (A) Coronal; and (B) sagittal images reveal that the PRMM (white arrow) consisted of a single fiber bundle, appeared as mixed signals, and inserted on the posterior slope of the medial tibial tubercle.

roots in this study were just an imaging classification and may not reflect the true constitution of the meniscal roots. However, this imaging classification is significant for radiologists to understand the normal imaging features of the meniscal roots on MRI.

Although this study participants were young asymptomatic volunteers, many high signals can be observed within the meniscal roots on the PDW MR. Increased signal intensity in the meniscal roots may be attributed to the following reasons. First,

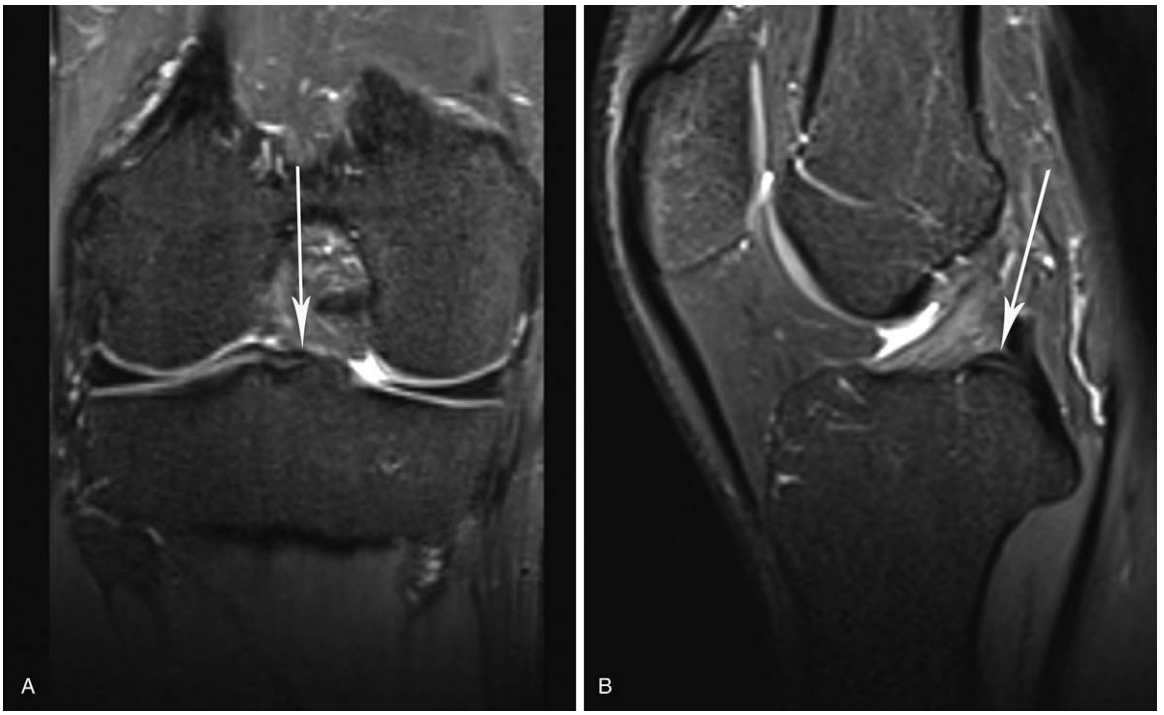

Figure 6. Posterior root of the lateral meniscus (PRLM). (A) Coronal; and (B) sagittal images reveal that the PRLM (white arrow) consisted of a single fiber bundle, appeared as hypointense, and inserted on the medial tibial tubercle along the intertubercular fossa.

Table 2

Constitution patterns of the meniscal roots on 3D PDW SPACE.

Meniscal root	Pattern	Constitution patterns	Percentage
ARMM	Type I	Consisted of a single fiber bundle (Fig. 1)	57 (95%)
	Type II	No insertion site on the tibial plateau; the transverse genual ligament was observed	2 (3.3%)
	Type III	Consisted of three fiber bundles	1 (1.7%)
ARLM		Consisted of multiple (≥3) fiber bundles (Fig. 2)	60 (100%)
PRMM	Type I	Consisted of multiple (≥3) fiber bundles (Fig. 3)	41 (68.3%)
	Type II	Consisted of 2 fiber bundles (Fig. 4)	14 (23.3%)
	Type III	Consisted of a single fiber bundle (Fig. 5)	5 (8.3%)
PRLM	Type I	One insertion site: consisted of a single fiber bundle (Fig. 7)	32 (53.3%)
	Type II	Two insertion sites: the major component consisted of a single fiber bundle and the minor component consisted of a single fiber bundle (Fig. 6)	25 (41.7%)
	Type III	Two insertion sites: the major component consisted of a single fiber bundle and the minor component consisted of 2 fiber bundles	3 (5%)

3D = 3-dimensional, ARLM = anterior root of the lateral meniscus, ARMM = anterior root of the medial meniscus, PDW = proton density-weighted, PRLM = posterior root of the lateral meniscus, PRMM = posterior root of the medial meniscus, SPACE = sampling perfection with application-optimized contrasts using different flip angle evolutions.

Table 3

MR signals of the meniscal roots on 3D PDW SPACE.

Meniscal root	Hypointense	Mixed signal	Hyperintense
ARMM	57 (95%) (Fig. 1)	3 (5%) [Stripe-like 1/3, 33.3%]	0
ARLM	0	60 (100%) [stripe-like 60/60, 100%] (Fig. 2)	0
PRMM	2 (3.3%) (Fig. 4)	55 (91.7%) [stripe-like 41/55, 74.5%] (Figs. 3 and 5)	3 (5%)
PRLM	46 (76.7%) (Figs. 6 and 7)	12 (20%)	2 (3.3%)

3D = 3-dimensional, ARLM = anterior root of the lateral meniscus, ARMM = anterior root of the medial meniscus, PDW = proton density-weighted, PRLM = posterior root of the lateral meniscus, PRMM = posterior root of the medial meniscus, SPACE = sampling perfection with application-optimized contrasts using different flip angle evolutions.

internal inherent components in the meniscal roots, which can appear as a high signal intensity on the PDW MR, are present. The meniscal roots are well-vascularized, similar to the red zone of the menisci,[18,19] and are known to have a fibrocartilaginous enthesis, which can demonstrate higher signal intensity on a PDW sequence.[20–22] Second, a PDW sequence with a short echo time is vulnerable to the magic angle phenomenon.[23] As the ARLM and the PRMM usually appeared as a fan-shaped band, and the PRMM was inserted on the posterior slope of the tibial tubercle, they exhibited inclined directions observed on the coronal and sagittal images, an angle of 45 degrees was easily formed with the main magnetic field direction. Third, the ARLM and the PRMM usually consisted of multiple fiber bundles was found in this study, which made them to exhibit stripe-like signals.

According to published criteria, 1 of the diagnosing standards for MRTs was that the abnormally increased signal intensity within the meniscal roots contacting the articular surface.[7–9] Although the study participants were young asymptomatic volunteers, many high signals can be observed within the meniscal roots and could reach the articular surfaces, particularly in the ARLM and the PRMM, with stripe-like signals on 3D PDW MR images. Therefore, the following points should be obeyed for diagnosing MRTs on MR: first, we should put more emphasis on the integrity and the morphologic changes of the meniscal roots, not just based on signal intensity. Second, if the high signals within the meniscal roots were not along the course of the meniscal roots, it may indicate MRTs. Third, the indirect signs of MRTs which include meniscal extrusion and parameniscal cysts can be used to aid in the identifcation of MRTs.[9]

This study has a number of limitations. First, although the study participants in this study were young asymptomatic volunteers, some congenital lesions without clinical symptoms may exist. Second, although we proposed some points for diagnosing MRTs on MR, the diagnostic criteria for MRTs is still need further refinement.

5. Conclusions

The study systematically evaluated the MR anatomy of the meniscal roots in young asymptomatic volunteers with a 3D MR. The 3D PDW SPACE sequence can excellently display the detailed anatomy of the meniscal roots. The meniscal roots can be complex and diverse, and certain characteristics of them were observed. Understanding the normal imaging features of the meniscal roots is extremely beneficial for further diagnosis of root tears.

Author contributions

Methodology: Ping Wang, Cheng-zhou Zhang, Di Zhang.
Resources: Quan-yuan Liu.
Supervision: Ping Wang, Xiao-fei Zhong, Zhi-jie Yin.
Writing – original draft: Ping Wang.
Writing – review & editing: Bin Wang.

Figure 7. Posterior root of the lateral meniscus (PRLM). (A) Posterior coronal; (B) anterior coronal; (C) lateral sagittal; and (D) medial sagittal images reveal 2 insertion sites of the PRLM: the major component (thick, white arrow) consisted of a single fiber bundle, appeared as hypointense, and inserted on the medial tibial tubercle along the intertubercular fossa; the minor component (thin, white arrow) consisted of a single fiber bundle, appeared as hypointense, and inserted on the posterior slope of the lateral tibial tubercle.

References

[1] Brody JM, Hulstyn MJ, Fleming BC, et al. The meniscal roots: gross anatomic correlation with 3-T MRI findings. AJR Am J Roentgenol 2007;188:446–50.

[2] Hussain ZB, Chahla J, Mandelbaum BR, et al. The role of meniscal tears in spontaneous osteonecrosis of the knee: a systematic review of suspected etiology and a call to revisit nomenclature. Am J Sports Med 2017;1: 363546517743734.

[3] Allaire R, Muriuki M, Gilbertson L, et al. Biomechanical consequences of a tear of the posterior root of the medial meniscus Similar to total meniscectomy. J Bone Joint Surg Am 2008;90:1922–31.

[4] LaPrade CM, Jansson KS, Dornan G, et al. Altered tibiofemoral contact mechanics due to lateral meniscus posterior horn root avulsions and radial tears can be restored with in situ pull-out suture repairs. J Bone Joint Surg Am 2014;96:471–9.

[5] LaPrade CM, Foad A, Smith SD, et al. Biomechanical consequences of a nonanatomic posterior medial meniscal root repair. Am J Sports Med 2015;43:912–20.
[6] Schillhammer CK, Werner FW, Scuderi MG, et al. Repair of lateral meniscus posterior horn detachment lesions: a biomechanical evaluation. Am J Sports Med 2012;40:2604–9.
[7] De Smet AA, Blankenbaker DG, Kijowski R, et al. MR diagnosis of posterior root tears of the lateral meniscus using arthroscopy as the reference standard. Am J Roentgenol 2009;192:480–6.
[8] LaPrade RF, Ho CP, James E, et al. Diagnostic accuracy of 3.0 T magnetic resonance imaging for the detection of meniscus posterior root pathology. Knee Surg Sports Traumatol Arthrosc 2015;23:152–7.
[9] Palisch AR, Winters RR, Willis MH, et al. Posterior root meniscal tears: preoperative, intraoperative, and postoperative imaging for transtibial pullout repair. Radiographics 2016;36:1792–806.
[10] Cruz RS, Ferrari MB, Metsavaht L, et al. Understanding posterior meniscal roots lesions: from basic science to treatment. Rev Bras Ortop 2017;52:463–72.
[11] Ren AH, Zheng ZZ, Shang Y, et al. An anatomical study of normal meniscal roots with isotropic 3D MRI at 3 T. Eur J Radiol 2012;81:783–8.
[12] You MW, Park JS, Park SY, et al. Posterior root of lateral meniscus the detailed anatomic description on 3T MRI. Acta Radiol 2014;55: 359–65.
[13] Notohamiprodjo M, Horng A, Pietschmann MF, et al. MRI of the knee at 3 T: first clinical results with an isotropic PDfs-weighted 3D-TSE-sequence. Invest Radiol 2009;44:585–97.
[14] Johannsen AM, Civitarese DM, Padalecki JR, et al. Qualitative and quantitative anatomic analysis of the posterior root attachments of the medial and lateral menisci. Am J Sports Med 2012;40:2342–7.
[15] Johnson DL, Swenson TM, Livesay GA, et al. Insertion-site anatomy of the human menisci gross, arthroscopic, and topographical anatomy as a basis for meniscal transplantation. Arthroscopy 1995;11:386–94.
[16] Kohn D, Moreno B. Meniscus insertion anatomy as a basis for meniscus replacement: a morphological cadaveric study. Arthroscopy 1995;11: 96–103.
[17] Anderson CJ, Ziegler CG, Wijdicks CA, et al. Arthroscopically pertinent anatomy of the anterolateral and posteromedial bundles of the posterior cruciate ligament. J Bone Joint Surg Am 2012;94:1936–45.
[18] Gray JC. Neural and vascular anatomy of the menisci of the human knee. J Orthop Sports Phys Ther 1999;29:23–30.
[19] Longo UG, Campi S, Romeo G, et al. Biological strategies to enhance healing of the avascular area of the meniscus. Stem Cells Int 2012;2012:528359.
[20] Benjamin M, Milz S, Bydder GM. Magnetic resonance imaging of entheses. Part 1. Clin Radiol 2008;63:691–703.
[21] Benjamin M, Milz S, Bydder GM. Magnetic resonance imaging of entheses. Part 2. Clin Radiol 2008;63:704–11.
[22] Chang EY, Biswas R, DiCamillo P, et al. Morphologic characterization of meniscal root ligaments in the human knee with magnetic resonance microscopy at 11.7 and 3 T. Skeletal Radiol 2014;43:1395–402.
[23] Li T, Mirowitz SA. Manifestation of magic angle phenomenon comparative study on effects of varying echo time and tendon orientation among various MR sequences. Magn Reson Imaging 2003;21:741–4.